

A photometric study of two neglected eclipsing binaries

V. Kudak¹, M. Fedurco², V. Perig¹ and Š. Parimucha²

¹ Laboratory of Space Researches, Uzhhorod National University, Uzhhorod, Daleka Str., 2A, 88000, Ukraine;
lab-space@uzhnu.edu.ua

² Institute of Physics, Faculty of Science, University of P.J. Šafárik, Košice, Park Angelinum 9, 04001, Slovakia;
stefan.parimucha@upjs.sk

Received 2020 November 3; accepted 2021 February 18

Abstract We present the first *BVR* photometry, period variation and photometric light curve analysis of two poorly studied eclipsing binaries, V1321 Cyg and CR Tau. Observations were carried out from November 2017 to January 2020 at the observatory of Uzhhorod National University. Period variations were studied using all available early published as well as our minima times. We used the newly developed ELISa code for the light curve analysis and determination of photometric parameters for both systems. We found that V1321 Cyg is a close detached eclipsing system with a low photometric mass ratio of $q = 0.28$ which suggests that the binary is a post-mass transfer system. No significant period changes in this system are detected. CR Tau is, on the other hand, a semi-detached system where the secondary component almost fills its Roche lobe. We detected a long-term period increase at a rate of $1.49 \times 10^{-7} \text{ d yr}^{-1}$, which supports mass transfer from the lower mass secondary component to the more massive primary.

Key words: binaries: close — binaries: eclipsing — stars: individual (V1321 Cyg, CR Tau)

1 INTRODUCTION

Eclipsing binaries are an important group of variable stars, where both components are obscured from the observer during their mutual motion around a common center of mass. They exhibit features in their light curves (LCs), which are specific and well recognized among all variable stars. The shape of their LCs depends on the physical properties of the components and geometrical configuration (Hilditch 2001; Prša 2019). Analysis of LCs of eclipsing binaries can reveal, among other aspects, relative dimensions of stars, their effective temperatures, orbital inclination, eccentricity of the orbit and potential spots. Together with radial velocities obtained from spectroscopic observations, we can determine masses of the components, their distances and radii.

The shapes of components in binary stars are described by Roche geometry (Prša 2019). According to this, three configurations of binary systems are possible, detached (both components are in their Roche lobes), semi-detached (one component fills its Roche lobe) and contact, where both components overflow their Roche lobes. All this is reflected in the LCs and also has other observational consequences like a period change due to mass transfer,

angular momentum loss (e.g., Yang et al. 2009) and/or magnetic braking (Applegate 1992).

In this paper, we present photometry, period and LC analysis of two neglected detached binaries, which were, up to now, not studied in more detail in literature:

V1321 Cyg (NSVS 5731097) was mentioned as an eclipsing variable for the first time in Romano (1967). In the database of Kreiner (2004), the period of the system is listed as $P = 0.3640924 \text{ d}$. Otero et al. (2006) redefined the system as an Algol-type binary with an orbital period $P = 0.72818 \text{ d}$. In the catalog of Avvakumova et al. (2013), the orbital period of the system was again set to half of the previous value. The distance to the system is $735 \pm 12 \text{ pc}$ according to Gaia Data Release 2 (DR2) (Bailer-Jones et al. 2018).

CR Tau (GSC 01862–01633) was discovered by Hoffmeister (1949) who also determined ephemeris from minima times of photographic plates. The system was neglected till the paper from Agerer (1999), who presented the first CCD LC of the system and determined new ephemeris with period $P = 0.6827035 \text{ d}$. It is included in the catalog of Algol-type eclipsing binaries from Budding et al. (2004) and in the catalogs Malkov et al. (2006) and Avvakumova et al. (2013). This eclipsing

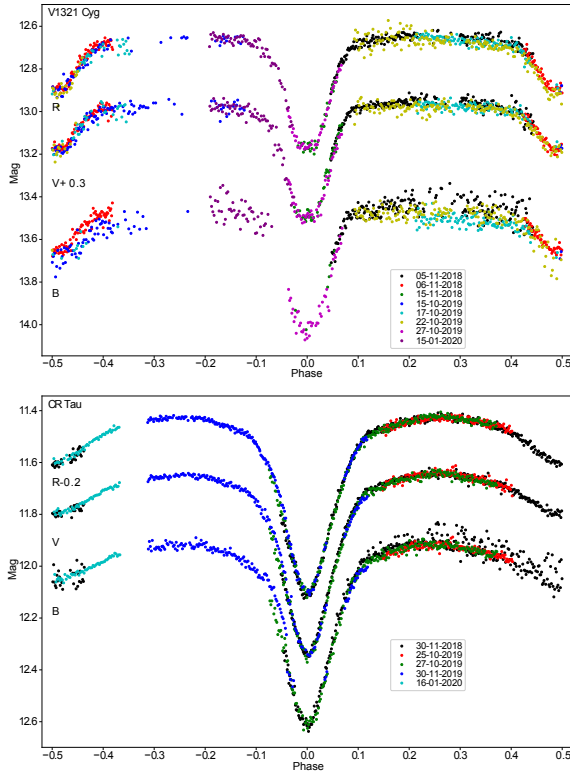


Fig. 1 Phased LC of the V1321 Cyg (*top*) and CR Tau (*bottom*) systems in *BVR* passbands by dates of observations.

binary was also monitored by the Optical Monitoring Camera (OMC) onboard the INTEGRAL satellite which provided photometry measurements in the Johnson *V*-band (Alfonso-Garzón et al. 2012). The distance to the system was established to be 796 ± 26 pc according to Gaia DR2 (Bailer-Jones et al. 2018).

2 OBSERVATIONS AND DATA REDUCTION

Observations of all studied eclipsing binary systems were carried out at Derenivka Observatory of Uzhhorod National University, Ukraine (Lat: 48.563417 N; Long: 22.453758 E). Measurements were collected from November 2017 to January 2020. For our observation, we employed a Newtonian telescope with a diameter of 400 mm and a focus of 1750 mm. It was accompanied by an FLI PL9000 CCD camera (array 3056×3056 , pixel size $12 \mu\text{m}$) with Johnson *BVR* photometric filters. The field of view of such configuration of the system is $1.21^\circ \times 1.21^\circ$. The journal of our CCD observations is given in Table 1.

The CCD images were reduced in the usual way (bias and dark subtraction, flat-field correction) utilizing the software package CoLiTecVS (Savanevych et al. 2017; Parimucha et al. 2019). This package was also used for aperture photometry, calculation of differential magnitudes

according to artificial comparison star as well as calibration to the standard photometric system. The comparison stars referenced for the determination of artificial ones were selected manually according to the similarity of the studied binaries (brightness and distance on the sky). This approach significantly improves the quality of photometric measurements. Due to not having stable night-to-night observing conditions, the average precision of our measurements reached ~ 0.02 mag in *V* and *R* filters and ~ 0.04 mag in *B* filter for CR Tau. Similarly, for the fainter binary V1321 Cyg, the average precision of individual measurements is a little worse, ~ 0.03 mag in *V* and *R* filters and ~ 0.05 mag in *B* filter. The comparison stars considered in our study together with their magnitudes from the NOMAD Catalog (Zacharias et al. 2004, 2005) are listed in Table 2.

The resulting LCs of all eclipsing binaries are depicted in Figure 1. The LCs were phased according to ephemeris determined from $O - C$ variations analyzed in the next section.

3 ANALYSIS OF PERIOD CHANGES

The study of period changes for both systems was carried out using their $O - C$ diagrams. In our analysis we have considered all available published minima times as can be found in the $O - C$ gateway¹, minima times determined from our observations (weighted averages from *BVR* LCs), minima times determined from available SuperWASP data (Pollacco et al. 2006) and INTEGRAL-OMC observations (Alfonso-Garzón et al. 2012). Our new minima times were calculated following the phenomenological method described in Mikulášek (2015). This method gives a realistic and statistically significant error in determining minima times. Newly calculated minima times are listed in Table 2.

The $O - C$ diagram of V1321 Cyg compiled from archived CCD and newly determined ones contains a total of 88 times of light minima. We have omitted old photographic minima times obtained before 1968 because of their large scatter. We also excluded visual observations. The precision of CCD minima times is in the range of 10^{-4} d. A weighted least-squares (LS) solution using all minima (weights were calculated as $1/\sigma^2$, where σ is an error in the minimum) leads to the following linear ephemeris of the system (errors of parameters are given in parentheses)

$$\text{Min I} = \text{HJD } 2458428.879(3) + 0^{\text{d}}.7281849(5) \times E. \quad (1)$$

This ephemeris was utilized to create the $O - C$ diagram displayed in Figure 2 (left). Despite the fact that we only used CCD observations, quite a large scatter in the

¹ <http://var2.astro.cz/ocgate/>

Table 1 The journal of CCD photometric observations. Phase is calculated according to ephemeris determined in Sect. 3.

System	Date	Time (UT)	Phase	Filters
V1321 Cyg	Nov 05 18	16:27 – 23:22	0.047 – 0.442	BVR
	Nov 06 18	16:32 – 19:55	0.426 – 6.618	BVR
	Nov 15 18	19:59 – 21:31	0.977 – 0.053	BVR
	Oct 15 19	17:09 – 23:56	0.500 – 0.882	BVR
	Oct 17 19	16:39 – 00:19	0.213 – 0.635	BVR
	Oct 22 19	16:54 – 01:02	0.093 – 0.544	BVR
	Oct 27 19	16:57 – 18:47	0.961 – 0.068	BVR
	Jan 15 20	16:40 – 20:04	0.808 – 0.971	BVR
CR Tau	Nov 30 18	18:31 – 04:31	0.945 – 0.562	BVR
	Oct 25 19	23:13 – 03:24	0.146 – 0.401	BVR
	Oct 27 19	20:45 – 04:02	0.927 – 0.371	BVR
	Nov 30 19	20:05 – 03:07	0.688 – 0.117	BVR
	Jan 16 20	19:37 – 21:43	0.503 – 0.634	BVR

Table 2 Comparison stars used for a determination of artificial comparison stars. BVR magnitudes are taken from the NOMAD Catalog (Zacharias et al. 2004, 2005)

System	Comparison stars NOMAD	Coordinates		B	V	R
		$\alpha(2000)$	$\delta(2000)$			
V1321 Cyg	1315–0399331	20:23:35.66	+41:32:52.8	14.780	14.330	15.240
	1315–0399475	20:23:48.84	+41:31:36.3	12.590	12.380	11.460
	1314–0397913	20:23:33.94	+41:27:56.5	14.190	13.680	14.240
	1315–0399386	20:23:41.82	+41:35:23.5	13.160	12.810	13.380
	1315–0399546	20:23:55.19	+41:30:28.6	15.140	14.520	14.950
CR Tau	1140–0090488	05:51:17.48	+24:04:56.1	12.456	12.072	10.95
	1140–0090531	05:51:21.78	+24:04:31.5	12.500	12.178	11.91
	1140–0090614	05:51:32.65	+24:04:55.0	14.813	14.101	13.41
	1141–0092118	05:51:38.19	+24:06:58.2	14.642	13.073	11.77

Table 3 New times of minima for studied objects. BVR - weighted average from our BVR LCs, SWASP - SuperWasp minima, OMC - INTEGRAL-OMC minima. The errors of minima times are given in parentheses.

HJD (2400000+)	Filter	HJD (2400000+)	Filter	HJD (2400000+)	Filter
V1321 Cyg		54371.4324(10)	SWASP	54070.6860(10)	SWASP
54278.5914(17)	SWASP	54394.3668(18)	SWASP	54118.4750(10)	SWASP
54279.6808(9)	SWASP	54398.3755(12)	SWASP	54179.5762(8)	OMC
54282.5926(9)	SWASP	58429.2438(4)	BVR	54141.3452(3)	SWASP
54298.6130(6)	SWASP	58774.4070(9)	BVR	54142.3747(9)	SWASP
54318.6419(10)	SWASP	58779.4987(4)	BVR	54143.3917(5)	SWASP
54335.3949(22)	SWASP	58784.2343(4)	BVR	54145.4408(9)	SWASP
54337.5702(21)	SWASP	CR Tau		55070.5057(2)	OMC
54339.3939(11)	SWASP	54030.7452(5)	SWASP	55454.1833(6)	OMC
54340.4820(29)	SWASP	54050.5426(9)	SWASP	55455.8888(2)	OMC
54344.4887(7)	SWASP	54056.6889(2)	SWASP	58453.3040(1)	BVR
54345.5821(29)	SWASP	54067.6108(4)	SWASP	58784.4165(1)	BVR
54363.4224(5)	SWASP	54069.6594(3)	SWASP	58818.5517(3)	BVR

resulting diagram is apparent in the range of about 10 min. However, no significant period changes in this system are detected.

The $O - C$ diagram of CR Tau contains 48 CCD times of minima, including archival and new points. We again excluded old photographic minima times obtained by Hoffmeister (1949), because of their very large scatter (up to 2 hr on the $O - C$ diagram). The precision of CCD minima times is in the range of 10^{-4} d. As in the previous case, we produced a weighted LS solution including all minima and determined the following linear ephemeris of

the system

$$\text{Min I} = \text{HJD } 2452500.125(3) + 0^{\text{d}}.6827039(4) \times E, \tag{2}$$

which was used to create the $O - C$ diagram depicted in Figure 2 (right). Unlike the previous case, there is some visible variation on the $O - C$ of CR Tau. Because of the lack of minima times and insufficient coverage, we can only speculate about their nature. The first explanation can be a mass transfer between components in the system. We calculated a weighted LS solution of residuals and

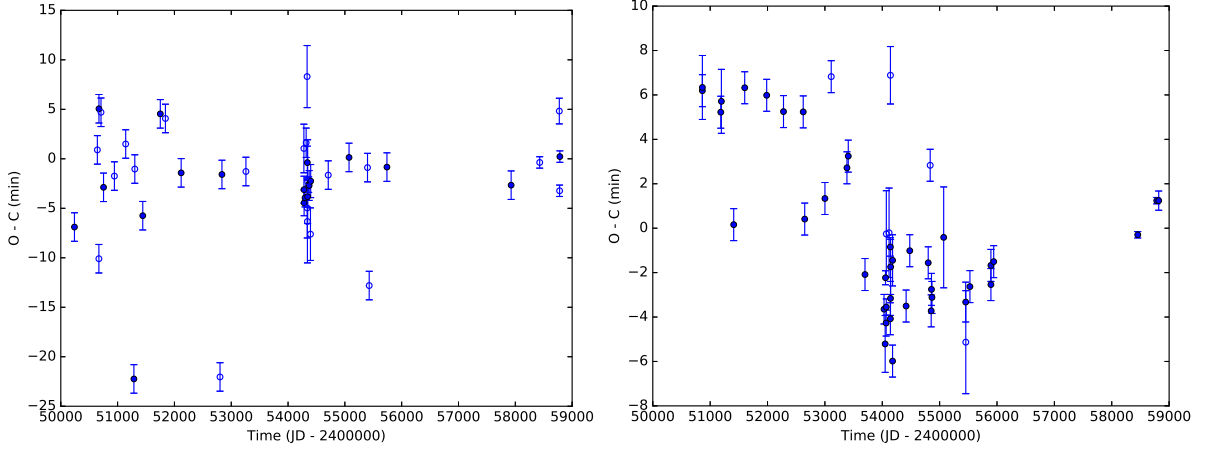


Fig. 2 $O - C$ diagrams of V1321 Cyg (*left*) and CR Tau (*right*) systems determined from linear ephemerides (1) and (2). Primary minima are signified by filled circles and secondary ones by blank circles.

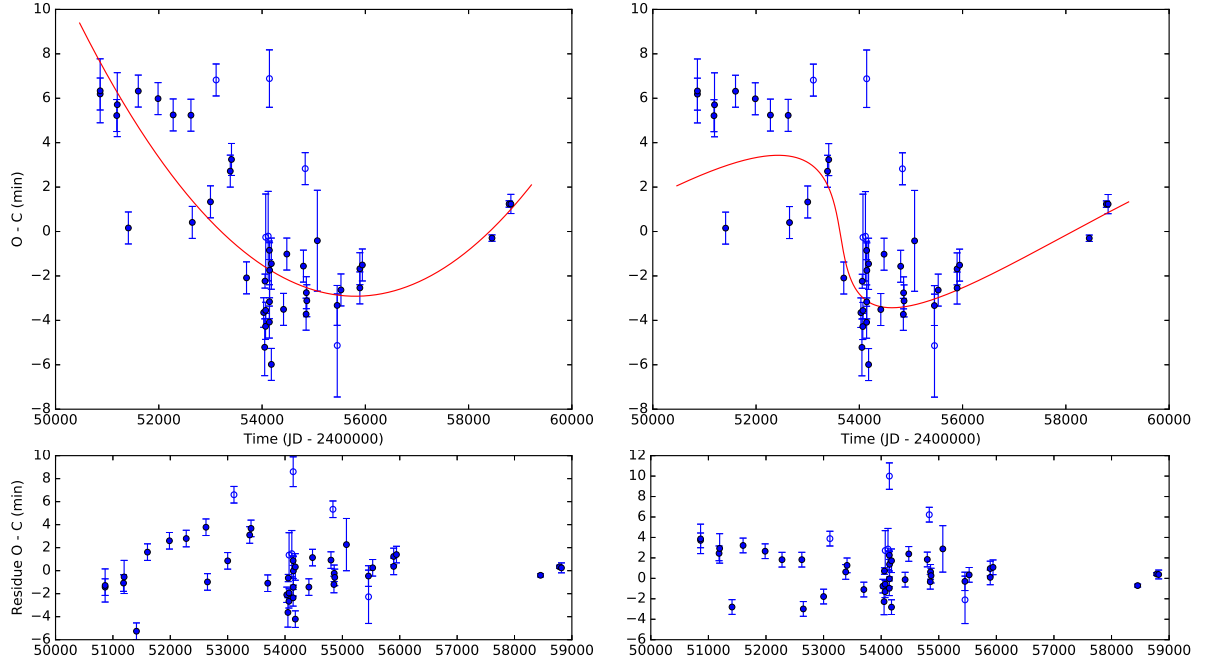


Fig. 3 The fit (*red line*) of the $O - C$ diagram of CR Tau systems according to a quadratic ephemeris (*left*) and 3rd body (*right*), with residuals at the bottom.

obtained the quadratic ephemeris

$$\begin{aligned} \text{Min I} = & \text{HJD } 2452500.1267(12) + 0^{\text{d}}.6827026(6) \times E \\ & + 1.395(64) \times 10^{-10} \times E^2. \end{aligned} \quad (3)$$

This solution is depicted in Figure 3 (left). According to ephemeris (3), a long-term period increase at a rate of $1.494(8) \times 10^{-7} \text{d yr}^{-1}$ is detected. The second possible explanation of the $O - C$ diagram is the presence of a 3rd body in the system, which we do not directly see. It causes a light-time effect, a shifting of minima times according to the movement of the visible binary around the common center of mass (Hilditch 2001). We have used code from Gajdoš & Parimucha (2019) to test this hypothesis. Our

best solution (displayed in Fig. 3 - right) led to the highly eccentric $e = 0.8$ orbit of the body with an orbital period of almost 28 yr.

4 LIGHT CURVE ANALYSIS

For the analysis of LCs of both systems, we relied on the ELISA² code (Čokina et al. 2021). It is a newly developed cross-platform Python software package dedicated to modeling close eclipsing binaries including surface features such as spots and pulsations. ELISA utilizes modern approaches to the EB modeling with an emphasis

² <https://github.com/mikecokina/elisa>

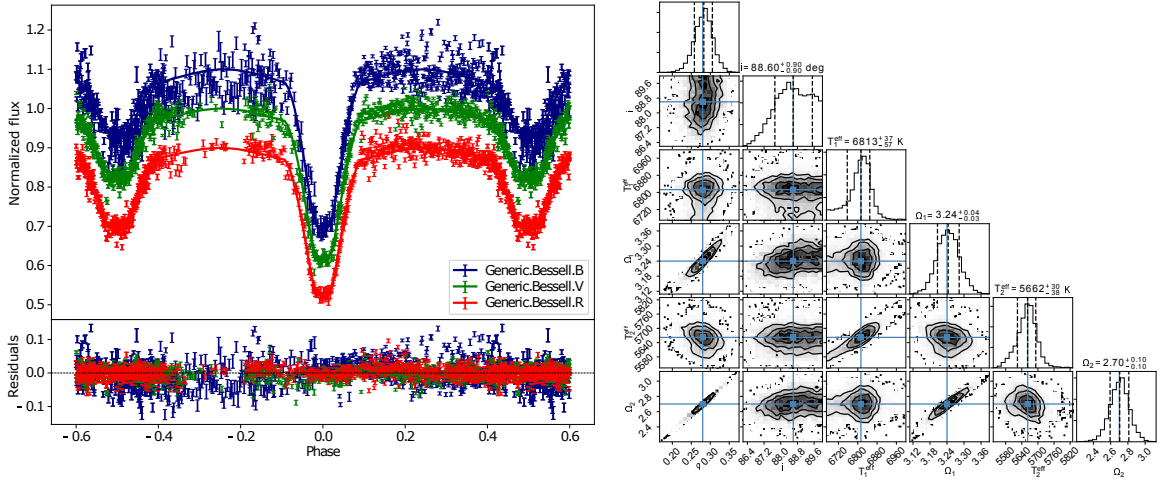


Fig. 4 The synthetic model fitted on observational data of V1321 Cyg (left) and the results of the MCMC sampling displayed in the form of the corner plot (right).

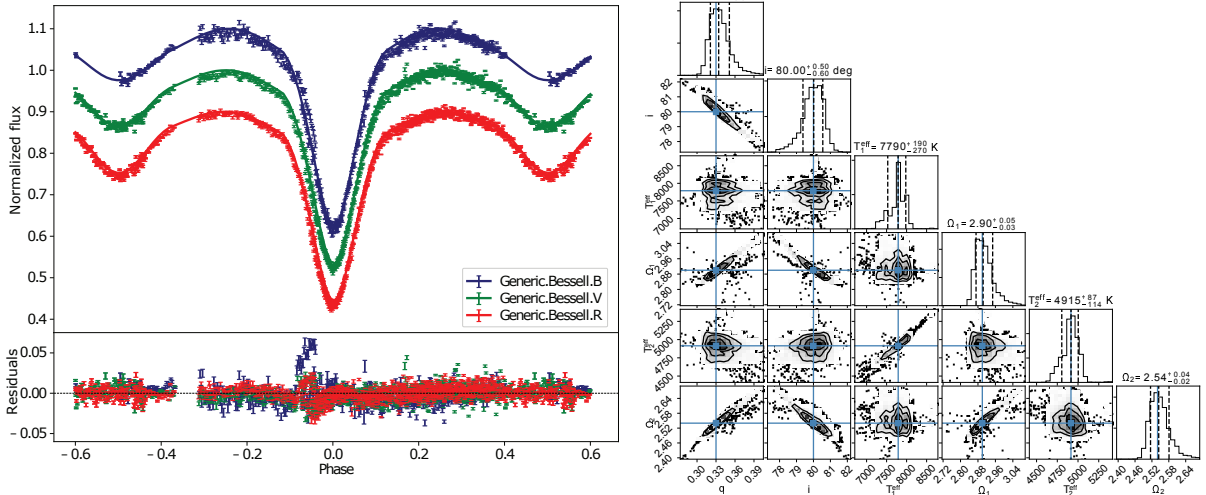


Fig. 5 The synthetic model fitted on observational data of CR Tau (left) and the results of the MCMC sampling displayed in the form of the corner plot (right).

on computational speed while maintaining a sufficient level of precision to process a ground-based and space-based observation. In this paper, we take advantage of its capability to model the LCs of close eclipsing binaries with the built-in capability to solve an inverse problem using the LS and Markov Chain Monte-Carlo (MCMC) methods.

Observations in all passbands were normalized according to flux in the maxima and were simultaneously fitted by the LS method to find initial approximate solutions. Subsequently, MCMC sampling was employed to produce 1σ confidence intervals of the fitted system parameters. Each system was fitted with a model containing six free parameters: orbital inclination i , photometric mass ratio q , surface potentials of both components Ω_1 and Ω_2 and effective temperatures of the primary and secondary components T_1^{eff} and T_2^{eff} respectively. In case

of V1321 Cyg, T_1^{eff} was kept within ± 300 K of the value 6770 K obtained from LAMOST spectra during the fitting procedure (Qian et al. 2018). On the other hand, T_1^{eff} of CR Tau was constrained within a ± 1000 K interval from the value 8200 K provided by Gaia DR2 (Gaia Collaboration et al. 2018).

For the components with convective envelopes (effective temperatures below ~ 7000 K), the albedos A_1 and A_2 of components were set to 0.6 (Ruciński 1969) and gravity darkening factors, g_1 and g_2 , to 0.32 (Lucy 1967). In the case of a radiative envelope (above ~ 7000 K), the values of albedo and gravity darkening factor were both set to 1.0. Castelli & Kurucz (2003) models of stellar atmospheres were applied. The linear limb darkening coefficients for each component were interpolated from the van Hamme (1993) tables.

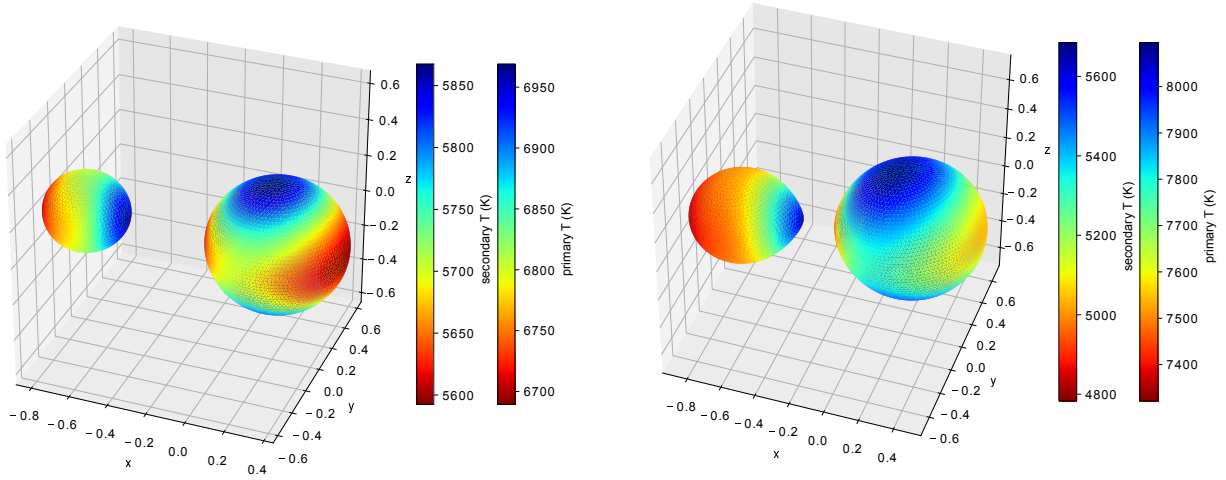


Fig. 6 Three-dimensional (3D) models with the most likely surface temperature distributions of V1321 Cyg (*left*) and CR Tau (*right*) binary systems based on parameters obtained from LC fitting listed in Table 4. The displayed temperature distributions take into account gravity darkening and the reflection effect using standard techniques based on the Wilson-Devinney code (Wilson & Devinney 1971).

The weights of individual data points were established as $1\sigma^2$, where σ is the standard error of a point derived during photometric measurement. Initially, the LS algorithm was used with suitable initial parameters to find an approximate solution and then the parameter space near the solution was explored with an MCMC sampler with 500 walkers and 500 iterations with the initial 300 iterations being discarded as they belonged to the thermalization stage of the sampling. The resulting and derived parameters of both systems, like a critical potential Ω_{crit} , corresponding radius R_{equiv} and periastron radii in Semi-major Axis (SMA), are listed in Table 4. The best-fit models with observed LCs and resulting flat chains displayed in the form of the corner plot are shown in Figures 4 and 5. In Figure 6 we also display 3D models of the systems with a temperature distribution, corresponding to a best fitting solution listed in Table 4.

5 DISCUSSION AND CONCLUSIONS

In our study we have presented the first multi-color *BVR* photometry of two, so far neglected, eclipsing binaries, V1321 Cyg and CR Tau. We have analyzed their period variations considering archival data and our new minima times as well as performing a photometric analysis of their LCs.

The analysis of our multi-color photometric observations demonstrates that V1321 Cyg is a close detached binary with a low photometric mass ratio of $q = 0.28^{+0.02}_{-0.03}$. Such a low value of q combined with a secondary potential $\Omega_2 = 2.7^{+0.1}_{-0.1}$ being relatively close to the critical potential $\Omega_{\text{crit},2} = 2.43^{+0.06}_{-0.06}$ suggests that V1321 Cyg is a post-mass transfer system, where a significant portion of the

secondary component’s mass was transferred onto the primary component. We detected no significant period changes in this system and it also supports the idea that the system is detached. We found two viable solutions, however only one was located within the temperature range derived by the LAMOST spectra while the second discarded solution contained a much colder primary component with ≈ 6000 K, well below the expected value.

On the other hand, a photometric analysis of the LCs of CR Tau revealed that the system is a semi-detached system where the secondary component almost fills its Roche lobe, as detected in some other near-contact systems, like EG Cep (Zhu et al. 2009) or BF Vir (Zhu et al. 2012). The main consequence of such a configuration is a mass transfer from the secondary to the primary component, which is reflected on the $O - C$ diagram as a parabolic variation according to the epoch. If the mass is transferred from a less massive star to a more massive one, we detect period increase, as observed in our data (see Fig. 3 - left). We can hence conclude that the most probable explanation for $O - C$ variations of CR Tau is a mass transfer and further observations should confirm that.

Subtraction of the best fit from the observed multi-color data (Fig. 5 - left) uncovered phase correlated residuals centered around the primary eclipse. This can also be explained by the mass transfer from the less massive and much cooler secondary component onto the heavier primary component. The surface of the primary component is obscured by a fraction of the relatively cold stream of matter from the secondary component. A slight shift in the position of residuals to the beginning of the eclipse can be explained by the Coriolis force acting

Table 4 Parameters of the V 1321 Cyg and CR Tau systems derived from multi-color photometry utilizing the ELISa code. The description of parameters is given in text. Goodness of the obtained fits are provided in the form of coefficient of determination R^2 .

Parameter	V1321 Cyg		CR Tau	
	Primary	Secondary	Primary	Secondary
P (HJD)	0.7281849 ^a		0.6827039 ^a	
T_0 (HJD)	2458428.879 ^a		2452500.125 ^a	
i (deg)	88.6 ^{+0.9} _{-0.9}		80.0 ^{+0.5} _{-0.7}	
q (M_2/M_1)	0.28 ^{+0.02} _{-0.03}		0.33 ^{+0.02} _{-0.01}	
T (K)	6810 ⁺⁴⁰ ₋₆₀	5660 ⁺³⁰ ₋₄₀	7790 ⁺¹⁹⁰ ₋₂₆₀	4916 ⁺⁸⁷ ₋₁₁₁
Ω	3.24 ^{+0.04} _{-0.04}	2.7 ^{+0.1} _{-0.1}	2.90 ^{+0.04} _{-0.03}	2.54 ^{+0.04} _{-0.03}
Ω_{crit}	2.43 ^{+0.05} _{-0.06}	2.43 ^{+0.06} _{-0.06}	2.54 ^{+0.04} _{-0.03}	2.54 ^{+0.04} _{-0.03}
$R_{\text{equiv}}(\text{SMA})$	0.343 ^{+0.002} _{-0.002}	0.214 ^{+0.002} _{-0.002}	0.401 ^{+0.003} _{-0.005}	0.288 ^{+0.004} _{-0.003}
Periastron radii (SMA)				
r_{polar}	0.336 ^{+0.002} _{-0.002}	0.207 ^{+0.001} _{-0.001}	0.386 ^{+0.003} _{-0.004}	0.2684 ^{+0.004} _{-0.003}
r_{backward}	0.350 ^{+0.002} _{-0.002}	0.222 ^{+0.003} _{-0.003}	0.414 ^{+0.003} _{-0.005}	0.3117 ^{+0.004} _{-0.003}
r_{side}	0.345 ^{+0.002} _{-0.002}	0.211 ^{+0.002} _{-0.002}	0.402 ^{+0.004} _{-0.005}	0.2794 ^{+0.004} _{-0.003}
r_{forward}	0.354 ^{+0.002} _{-0.002}	0.227 ^{+0.004} _{-0.004}	0.427 ^{+0.004} _{-0.005}	0.376 ^{+0.008} _{-0.010}
R^2	0.932		0.994	

^a - adopted values of period and epoch from linear ephemerides.

on the falling stream of matter. Additionally, it is worth mentioning other observed proximity effects such as the deformation and heating of the secondary component of CR Tau on the part of the surface facing the primary component due to the close proximity of the components and large temperature difference between the components' surfaces.

Acknowledgements This work was supported by national grant 0119U100236 and by the Slovak Research and Development Agency under contract No. APVV-15-0458. The research of M.F. was supported by the internal grant No. VVGS-PF-2019-1392 of the Faculty of Science, P. J. Šafárik University in Košice.

References

- Agerer, F. 1999, Information Bulletin on Variable Stars, 4778, 1
- Alfonso-Garzón, J., Domingo, A., Mas-Hesse, J. M., & Giménez, A. 2012, A&A, 548, A79
- Applegate, J. H. 1992, ApJ, 385, 621
- Avvakumova, E. A., Malkov, O. Y., & Kniazev, A. Y. 2013, Astronomische Nachrichten, 334, 860
- Bailer-Jones, C. A. L., Rybizki, J., Fousneau, M., et al. 2018, AJ, 156, 58
- Budding, E., Erdem, A., Çiçek, C., et al. 2004, A&A, 417, 263
- Castelli, F., & Kurucz, R. L. 2003, in Modelling of Stellar Atmospheres, ed. N. Piskunov, W. W. Weiss, & D. F. Gray, 210, A20
- Čokina, M., Fedurco, M., & Parimucha, Š. 2021, submitted
- Gaia Collaboration, Brown, A. G. A., Vallenari, A., et al. 2018, A&A, 616, A1
- Gajdoš, P., & Parimucha, Š. 2019, Open European Journal on Variable Stars, 197, 71
- Hilditch, R. W. 2001, An Introduction to Close Binary Stars (Cambridge Univ. Press)
- Hoffmeister, C. 1949, Erg. AN, 12, 1
- Kreiner, J. M. 2004, Acta Astronomica, 54, 207
- Lucy, L. B. 1967, ZAp, 65, 89
- Malkov, O. Y., Oblak, E., Snegireva, E. A., & Torra, J. 2006, A&A, 446, 785
- Mikulášek, Z. 2015, A&A, 584, A8
- Otero, S. A., Hoogeveen, G. J., & Wils, P. 2006, Information Bulletin on Variable Stars, 5674, 1
- Parimucha, Š., Savanevych, V. E., Briukhovetskyi, O. B., et al. 2019, Contributions of the Astronomical Observatory Skalnaté Pleso, 49, 151
- Pollacco, D. L., Skillen, I., Collier Cameron, A., et al. 2006, PASP, 118, 1407
- Prša, A. 2019, Modeling and Analysis of Eclipsing Binary Stars: The Theory and Design Principles of PHOEBE (Institute of Physics Publishing)
- Qian, S. B., Zhang, J., He, J. J., et al. 2018, ApJS, 235, 5
- Romano, G. 1967, Information Bulletin on Variable Stars, 229, 1
- Ruciński, S. M. 1969, Acta Astronomica, 19, 245
- Savanevych, V. E., Briukhovetskyi, O. B., Khlamov, S. V., et al. 2017, Odessa Astronomical Publications, 30, 194
- van Hamme, W. 1993, AJ, 106, 2096
- Wilson, R. E., & Devinney, E. J. 1971, ApJ, 166, 605
- Yang, Y. G., Lü, G. L., Yin, X. G., et al. 2009, AJ, 137, 236
- Zacharias, N., Monet, D. G., Levine, S. E., et al. 2004, in American Astronomical Society Meeting Abstracts, 205, 48.15
- Zacharias, N., Monet, D. G., Levine, S. E., et al. 2005, VizieR Online Data Catalog, I/297
- Zhu, L., Qian, S.-B., & Li, L. 2012, PASJ, 64, 94
- Zhu, L. Y., Qian, S. B., Liao, W. P., Zejda, M., & Mikulášek, Z. 2009, PASJ, 61, 529